# Theoretical and Experimental Study on Phase Transitions and Mass Fluxes of Supersaturated Water Vapor onto Different Insoluble Flat Surfaces

Antti Lauri,*,† Ilona Riipinen,† Jukka A. Ketoja,‡ Hanna Vehkamäki,† and Markku Kulmala†

*Department of Physical Sciences, University of Helsinki, P.O. Box 64, FI-00014 Helsinki, Finland, and KCL Science and Consulting, P.O. Box 70, FI-02151 Espoo, Finland*

*Received July 17, 2006. In Final Form: September 6, 2006*

The heterogeneous nucleation and condensation of water vapor onto three different surfaces (newsprint paper, Teflon, cellulose film) was studied theoretically and experimentally. The theoretical framework included the use of the classical theory of heterogeneous nucleation, diffusion theory corrected with transition regime correction factors, and the theory of heat transfer. Experiments were carried out using an environmental scanning electron microscope (ESEM). The experimental results for newsprint paper were investigated more closely. Our results show that the measured onset supersaturations were smaller than the modeled ones when the experimentally determined contact angle was used. Furthermore, the measured condensational growth rates were smaller than the modeled ones, presumably resulting from the approximations that had to be made in the calculations.

## 1. Introduction

The formation of liquid embryos on insoluble surfaces from supersaturated vapors and the subsequent growth of these embryos to observable droplets represents an everyday phenomenon. An important industrial application of condensation is in paper-making, where a smoother and glossier paper surface is achieved by moistening the surface before the so-called calendering operation.[1] This technique is applied at almost any paper mill. Still, the water-transfer mechanisms are poorly understood.

The processes present in the phenomenon are illustrated in Figure 1. In the initial situation, there is supersaturated vapor and a surface. Vapor molecules form small embryos on the surface (Figure 1a). Some of the embryos grow to a thermodynamically stable size, causing the formation of a new liquid phase via heterogeneous nucleation (Figure 1b). Formed embryos start to grow when vapor condenses into them (Figure 1c). Droplets near each other may coalesce, forming larger droplets (Figure 1d). If the underlying surface is porous, then both vapor and liquid molecules will be absorbed into the surface. In this study, we approach the problem using theories of nucleation and condensation for one component vapor. Absorption and coalescence are not considered.

Lately, nucleation phenomena have been studied using different approaches (e.g. density functional theory[2−4] based on capillarity theory,[5] Monte Carlo simulations,[6−8] and molecular dynamics[9,10]). However, classical nucleation theory,[11−14] first presented for heterogeneous nucleation on flat surfaces first by Volmer,[15] is still the only one applicable for more complex situations.

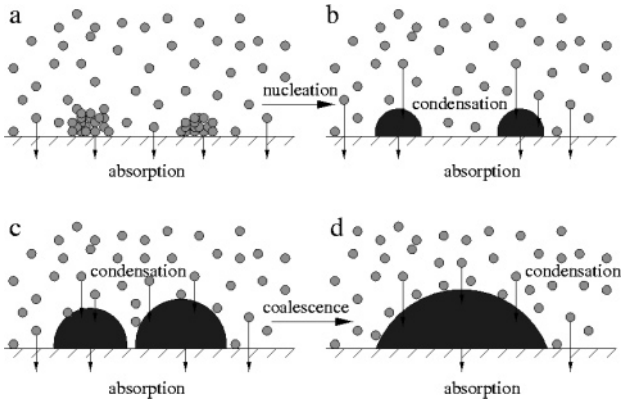


**Figure 1.** Processes involved in vapor condensing onto an insoluble surface. See the text for details.

Condensational growth follows right after nucleation because the vapor will prevail over supersaturation. The basic principles of the condensational growth of spherical droplets are theoretically rather well understood, and accurate expressions for the condensational mass and heat fluxes for both kinetic ($Kn \gg 1$) and continuum ($Kn \ll 1$) regimes are available.[16−19] In this work, however, we study sessile droplets with the shape of a spherical cap on different surfaces. Picknett and Bexon[20] derived a solution for the condensation/evaporation flux for such a droplet, using the analogy between diffusive concentration fields and the electrostatic potential field. The evaporation of sessile droplets on insoluble surfaces has also been studied by Deegan et al.,[21]

† University of Helsinki.
‡ KCL Science and Consulting.

(1) Bos, J. H., Veenstra, P., Verhoeven, H., de Vos, P. D., Eds. *Handbook of Papermaking*; ECA Pulp and Paper: Houten, The Netherlands, 1999.
(2) Zeng, X. C.; Oxtoby, D. W. *J. Chem. Phys.* **1991**, *95*, 5940−5947.
(3) Talanquer, V.; Oxtoby, D. W. *J. Chem. Phys.* **1997**, *106*, 3673−3680.
(4) Napari, I.; Laaksonen, A. *J. Chem. Phys.* **1999**, *111*, 5485−5489.
(5) Rowlinson, J.; Widom, B. *Molecular Theory of Capillarity*; Clarendon Press: Oxford, U.K., 1989.
(6) ten Wolde, P. R.; Frenkel, D. *J. Chem. Phys.* **1998**, *109*, 9901−9918.
(7) Oh, K.; Zeng, X. *J. Chem. Phys.* **1999**, *110*, 4471−4476.
(8) Merikanto, J.; Vehkamäki, H.; Zapadinsky, E. *J. Chem. Phys.* **2004**, *121*, 914−924.
(9) Laasonen, K.; Wonczak, S.; Strey, R.; Laaksonen, A. *J. Chem. Phys.* **2000**, *113*, 9741−9747.
(10) Toxvaerd, S. *J. Chem. Phys.* **2001**, *115*, 8913−8920.
(11) Volmer, M.; Weber, A. *Z. Phys. Chem.* **1925**, *119*, 277−301.
(12) Farkas, L. *Z. Phys. Chem.* **1927**, *125*, 236−242.
(13) Becker, R.; Döring, W. *Ann. Phys. (Leipzig)* **1935**, *24*, 719−752.
(14) Zeldovich, J. *Zh. Eksp. Theor. Fiz.* **1942**, *12*, 525−538.
(15) Volmer, M. *Kinetik der Phasenbildung*; Steinkopff: Dresden, Germany, 1939.
(16) Wagner, P. E. Aerosol Growth by Condensation. In *Aerosol Microphysics II*; Marlow, W. H., Ed.; Springer: Berlin, 1982.
(17) Barrett, J. C.; Clement, C. F. *J. Aerosol Sci.* **1988**, *19*, 223−242.
(18) Kulmala, M.; Vesala, T. *J. Aerosol Sci.* **1991**, *22*, 337−346.
(19) Kulmala, M. *Aerosol Sci. Technol.* **1993**, *19*, 381−388.
(20) Picknett, R. G.; Bexon, R. *J. Colloid Interface Sci* **1977**, *61*, 336−350.

10.1021/la062073n CCC: $33.50 
Published on Web 10/25/2006

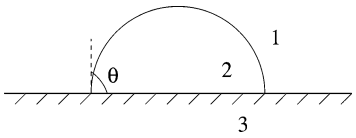


**Figure 2.** Contact angle of a liquid droplet on a flat insoluble surface. Phases are indicated by numbers: (1) surrounding vapor, (2) liquid droplet, and (3) underlying insoluble surface. The droplet is thought to be part of a sphere.

Cachile et al.,[22] and Hu and Larson.[23−25] Particularly for nonabsorbing surfaces and isothermal conditions, rather good agreement between theory and observations has been reported. In this study, we use the approach presented by Picknett and Bexon[20] corrected with transitional correction factors in an attempt to model the condensational growth of sessile water droplets on a newsprint paper surface.

## 2. Theory

Theoretical calculations consisted of two parts. The formation of liquid embryos was modeled using the classical theory of heterogeneous nucleation. Further condensational growth of the droplets was estimated using diffusion theory in the transition regime[18,19,26] and taking into account the concentration profile resulting from the lens-type shape of the droplets.[20] Heat fluxes were studied using formulations reported by Wagner[16] and Vesala et al.[27]

**2.1. Heterogeneous Nucleation.** We have followed the ideas of the classical theory of heterogeneous nucleation, first introduced for flat surfaces by Volmer.[15] In this formulation, the critical embryos forming on the surface are considered to be segments of a sphere, each having the same radius and contact angle (Figure 2). The classical theory relies on the use of macroscopically determined bulk properties for the critical cluster. The capillarity approximation is used for the surface tension: the surface tension of a flat surface is used for the embryo. The liquid density is taken to be that of the incompressible liquid. Other physicochemical properties needed for the calculations include the contact angle and the saturated vapor pressure.

In the case of heterogeneous nucleation, geometry plays a major role. The embryo is represented by a segment of a sphere, contacting the flat surface by angle $\theta$, which is called the contact angle (Figure 2). In the Figure, the vapor phase is denoted by 1, the liquid embryo, by 2, and the insoluble flat surface, by 3. The system has to pass the energy barrier described by the Gibbs free energy for the phase transition to occur. The Gibbs free energy for embryo formation on an insoluble surface in the general case is given by

$$\Delta G = \Delta G_v V + \sigma_{12}A_{12} + (\sigma_{23} - \sigma_{13})A_{23} \qquad (1)$$

where $\Delta G_v$ is the free energy difference per unit volume of embryo between matter in the parent phase and matter in the embryo phase, $V$ is the volume of the embryo, $A_{ij}$ is the surface area separating phases $i$ and $j$, and $\sigma_{ij}$ is the interfacial free energy between phases $i$ and $j$ as denoted in Figure 2. To apply equilibrium thermodynamics, we have to identify the equilibrium embryo size by locating the maximum point of the energy barrier:

$$\frac{\partial \Delta G}{\partial r}\Big|_{r^*} = 0 \qquad (2)$$

Choosing the dividing surface between the liquid and vapor phases so that it coincides with the surface of tension,[28] we can find the radius of the embryo using the Kelvin equation

$$\Delta\mu + \frac{2\sigma v_l}{r^*} = 0 \qquad (3)$$

where $\Delta\mu = \mu_l(T, P_v) - \mu_v(T, P_v)$ with $\mu_l$ and $\mu_v$ denoting the liquid- and vapor-phase chemical potentials, respectively, and $v_l(T)$ is the molecular volume of the liquid. The liquid is assumed to be incompressible. From eq 3, we are able to determine the critical radius of the forming embryos, knowing that for a one-component ideal gas

$$\Delta\mu = -kT \ln S \qquad (4)$$

where $S$ is the saturation ratio of the nucleating vapor. Because we are applying equilibrium thermodynamics, we assume that all of the forming embryos are of the same size. Now the critical free energy for the embryo formation is given by

$$\Delta G^* = \frac{4}{3}\pi r^{*2}\sigma_{12} f(m) \qquad (5)$$

where $f(m)$ is a geometrical term depending on the contact angle through $m = \cos\theta$

$$f(m) = \frac{(2 + m)(1 - m)^2}{4} \qquad (6)$$

The nucleation rate can be expressed as[29,30]

$$I = R_{av} F Z \exp\left(-\frac{\Delta G^*}{kT}\right) \qquad (7)$$

where $R_{av}$ is the average condensation rate, $Z$ is the Zeldovich nonequilibrium factor, and $F$ is the total number of nucleating molecules, clusters, particles, and so forth depending on the system under consideration. In homogeneous nucleation, $F$ would be the total number of molecules in the vapor. For heterogeneous nucleation, several different expressions for $F$ can be found in the literature.

In the formulation that we have used, nucleation is thought to proceed via direct vapor deposition. The approach takes into account only the monomer collisions hitting and adhering to the surface of the embryo. The other widely used approach to heterogeneous nucleation is the surface diffusion. In this approach, the collisions and adhering monomers on the substrate surface are also taken into account. Thus, the nucleation rate includes both the direct collisions of monomers on the embryo and the diffusion of the monomers on the substrate surface into the embryo. For the nucleation rate, we use

$$I = N^{ads} R_{av} Z \exp\left(\frac{-\Delta G^*}{kT}\right) \qquad (8)$$

The adsorption mechanism is included in the nucleation rate calculation by the number of molecules adsorbed on the surface

(21) Deegan, R. D.; Bakajin, O.; Dupont, T. F.; Huber, G.; Nagel, S. N. *Nature (London)* **1997**, *389*, 827−829.
(22) Cachile, M.; Bénichou, O.; Cazabat, A. M. *Langmuir* **2002**, *18*, 7985−7990.
(23) Hu, H.; Larson, R. G. *J. Phys. Chem. B* **2002**, *106*, 1334−1344.
(24) Hu, H.; Larson, R. G. *Langmuir* **2005**, *21*, 3963−3971.
(25) Hu, H.; Larson, R. G. *Langmuir* **2005**, *21*, 3972−3980.
(26) Bird, R. B.; Steward, W. E.; Lightfoot, E. N. *Transport Phenomena*; Wiley: New York, 1960.
(27) Vesala, T.; Kulmala, M.; Rudolf, R.; Vrtala, A.; Wagner, P. E. *J. Aerosol Sci.* **1997**, *28*, 565−598.
(28) Abraham, F. F. *Homogeneous Nucleation Theory*; Academic Press: New York, 1974.
(29) Stauffer, D. *J. Aerosol Sci.* **1976**, *7*, 319−333.
(30) Kulmala, M.; Laaksonen, A. *J. Chem. Phys.* **1990**, *93*, 696−701.

of an embryo

$$N^{\text{ads}} = \beta\tau \tag{9}$$

where $\beta$ is the impinging rate of vapor molecules on the embryo surface, interpreted as the condensation rate, and $\tau$ is the time the molecule spends on the surface (residence time), given by

$$\tau = \tau_0 \exp\left(\frac{E}{RT}\right) \tag{10}$$

where $\tau_0$ is a characteristic time and $E$ is the heat of adsorption. Lazaridis et al.[31] used the latent heat of condensation given by Adamson[32] for the heat of adsorption. The characteristic time can be determined by knowing the characteristic frequency of vibration $\nu_0$[32]

$$\tau_0 = \frac{1}{\nu_0} \tag{11}$$

The vibrational frequency is usually calculated using the nearest-neighbor harmonic oscillator approximation. For the water−water interaction, $\tau_0 = 2.55 \times 10^{-13}$ s.

**2.2. Condensation and Heat Fluxes.** First, we assumed the gas phase to consist only of water vapor (i.e., no carrier gas was present). In this case, the mass fluxes of water vapor to/from the spherical cap-shaped droplets can be calculated using the expression[18,20,26]

$$J = \frac{2rg(\theta)\beta_m\sqrt{\pi kM}}{3\pi {d_{\text{mol}}}^2} \frac{T_\infty - T_a}{\sqrt{T_\infty} - \sqrt{T_a}} \ln\left(\frac{p_{v\infty}T_a}{p_{va}T_\infty}\right) \tag{12}$$

where $r$ is the radius of the growing droplet (the droplet base has the radius $r \sin\theta$), $\beta_m$ is the transitional-regime correction factor, $M$ is the molecular mass, and $d_{\text{mol}}$ is the molecular diameter of the condensing vapor. $T_a$ and $T_\infty$ and similarly $p_{va}$ and $p_{a\infty}$ refer to vapor temperatures and pressures at the droplet surface and far away from droplet, respectively. The droplet is assumed to be in the steady state; therefore, $p_{va}$ equals the equilibrium vapor pressure of water on a liquid surface with curvature $r$. $g(\theta)$ is a geometrical factor taking into account the concentration profile in the vicinity of the sessile droplet and has the contact-angle-dependent form[20]

$$g(\theta) = 0.00008957 + 0.6333\theta + 0.1160\theta^2 - 0.08878\theta^3 + 0.010330\theta^4 \tag{13}$$

for contact angles larger than 0.175 rad (10°). Equation 12 is simply an integrated form of Fick's first law in a one-vapor system, taking into account the temperature and pressure dependencies of the self-diffusion coefficient $D_{ww}$, expressed as[26]

$$D_{ww} = \frac{2}{3}\left(\frac{k^3}{\pi^3 M}\right)^{1/2} \frac{T^{3/2}}{p{d_{\text{mol}}}^2} \tag{14}$$

To take into account the experimental uncertainties, we also studied the water vapor condensation in a gas−vapor mixture at a maximum 5 Torr of air. In this case, the mass flux to the droplet was calculated with[18,27]

$$J = \frac{4\pi rg(\theta)D_{w,air}\beta_m pM}{kT_\infty} C \ln\left(\frac{1 - (p_{va}/p)}{1 - (p_{v\infty}/p)}\right) \tag{15}$$

where $p$ refers to the total pressure in the experimental chamber, $g(\theta)$ is the geometrical factor described above, and $D_{w,air}$ refers now to the diffusion coefficient of water vapor in air, expressed as

$$D_{w,air}(T) = D_{w,air,N}\frac{p_N}{p}\left(\frac{T}{T_N}\right)^\mu \tag{16}$$

where the subsript $N$ points to a reference state (here 273 K and 1 atm). For water vapor, $D_{w,air,N} = 22.07487 \times 10^{-6}$ m$^2$/s and $\mu = 1.6658$.[33] The factor $C$ results from the temperature dependency of the diffusion coefficients and is of the form[18]

$$C = \frac{T_\infty - T_a}{T_\infty^{\mu-1}} \frac{2-\mu}{T_\infty^{2-\mu} - T_a^{2-\mu}} \tag{17}$$

The presence of the carrier gas gives rise to the so-called Stefan flux, which, in the case of condensation, is directed toward the droplet.

The droplet surface was assumed to exchange heat with the surrounding gas as well as the droplet base, which was assumed to have the temperature of the substrate (newsprint paper). The radiative heat transport was also taken into account for completeness. The total heat flux from the droplet surface can thus expressed as

$$Q = Q_{va} + Q_{ab} + Q_{rad} \tag{18}$$

where the subscripts v, a, b, and rad refer to vapor, droplet surface, droplet base, and radiation, respectively. The heat flux between the droplet surface and the gas phase was calculated with[16]

$$Q_{va} = 2\pi rg(\theta)\,\beta_T(k_{ga} + k_{g\infty})(T_a - T_\infty) - H_v J \tag{19}$$

where $k_{ga}$ and $k_{g\infty}$ are the thermal conductivities of the gas phase at the droplet surface and far away from the droplet, respectively. $H_v$ is the specific enthalpy on the condensing vapor, $J$ is the mass flux to the droplet (calculated with eq 12 or 15), and $\beta_T$ is the transitional correction factor for heat flux. The heat transfer between the droplet surface and its base was estimated with

$$Q_{ab} = \pi r^2 \sin^2\theta\, k_l \frac{T_a - T_b}{r(1-m)} \tag{20}$$

where $k_l$ is the thermal conductivity of the liquid water ($r^2 \sin^2\theta$ refers now to the droplet base area) and $T_b$ refers to the temperature of the substrate. The radiative flux from the droplet was calculated according to the Stéfan−Boltzmann law

$$Q_{rad} = 2\pi r^2(1-m)\sigma_b {T_a}^4 \tag{21}$$

where $\sigma_b$ is the Stéfan−Boltzmann coefficient. For the thermal conductivities of vapor and liquid water in units of W/m/K, we used the temperature-dependent expressions[33,34]

$$k_g = -6.7194 \times 10^{-3} + 7.4857 \times 10^{-5} T \tag{22}$$

$$k_l = -0.2758 + 4.6120 \times 10^{-3} T - 5.5391 \times 10^{-6} T^2 \tag{23}$$

(31) Lazaridis, M.; Kulmala, M.; Laaksonen, A. *J. Aerosol Sci.* **1991**, *22*, 823−830.

(32) Adamson, A. W. *Physical Chemistry of Surfaces*, 4th ed.; Wiley: New York, 1982.

In the case of the air−vapor mixture, we calculate the thermal conductivity of the mixture as described by Lindsay and Bromley.[35]

The transitional correction factors for mass and heat fluxes were expressed according to Fuchs and Sutugin[36]

$$\beta_m = \frac{1 + Kn}{1 + \left(\frac{4}{3\alpha_m} + 0.377\right)Kn + \frac{4}{3\alpha_m}Kn^2} \quad (24)$$

$$\beta_T = \frac{1 + Kn_T}{1 + \left(\frac{4}{3\alpha_T} + 0.377\right)Kn_T + \frac{4}{3\alpha_T}Kn_T^2} \quad (25)$$

where $Kn$ is the Knudsen number of the droplet defined as the ratio between the mean free path of the vapor/gas and the droplet radius. $\alpha_m$ and $\alpha_T$ are the mass and thermal accommodation coefficients. Both accommodation coefficients for water vapor as well as the thermal accommodation coefficient for air were assumed to be unity.

The temporal evolution of the condensation process was calculated by numerically solving coupled differential equations for the droplet mass and temperature as well as the ambient temperature and vapor concentration (e.g., Vesala et al.[27]).

## 3. Experiments

The aim of the experiments was to systematically determine the onset of heterogeneous nucleation as well as the contact angle and condensation rate of supersaturated vapor on different surfaces under controlled conditions. An environmental scanning electron microscope (ESEM) was used to study the phenomena. The ESEM chamber contained practically no air (at maximum 5 Torr), and the vapor was at room temperature (20 °C).

Three different samples including newsprint paper, Teflon, and cellulose film were used in the experiments. Newsprint was chosen because of its practical relevance in calendering operations. The samples were first cooled to 2−8 °C using an underlying Peltier device. Because of the high thermal conductivity of the samples,[37] we could expect the surface temperatures to stay close to their targets throughout the experiments. In the case of newsprint paper, the relative humidity was first increased to 100% for 90 s and was kept at the saturated vapor pressure for at least 10 min, allowing the fibers to absorb as much moisture as possible. After this prewetting period, the relative humidity was increased slowly (0.5−1%/min) until droplet formation was observed. This threshold pressure value, corresponding to the onset of heterogeneous nucleation, was recorded, and the amount of vapor was increased no further during the rest of the experiment. Condensational growth rates for the droplets were obtained from the ESEM pictures taken at 30 s intervals.

The microscopic contact angle for newsprint was measured by repeating the experiment with a tilted viewing angle and measuring the angle with visual inspection from the ESEM figures. We followed a few droplets and noticed that despite fluctuations, the average contact angle remained practically constant over extended time periods (e.g., 200 s). Moreover, the contact angle appeared to be quite independent of the chosen droplet.

The largest uncertainty in the experiments was related to the amount of air in the chamber. The secondary pumping action reduced the amount of air during the experiments.[38] At the threshold vapor pressure for nucleation, the amount of air was probably small but not necessarily insignificant. This means that the measured thresholds give essentially the upper boundary of critical water vapor pressure levels.

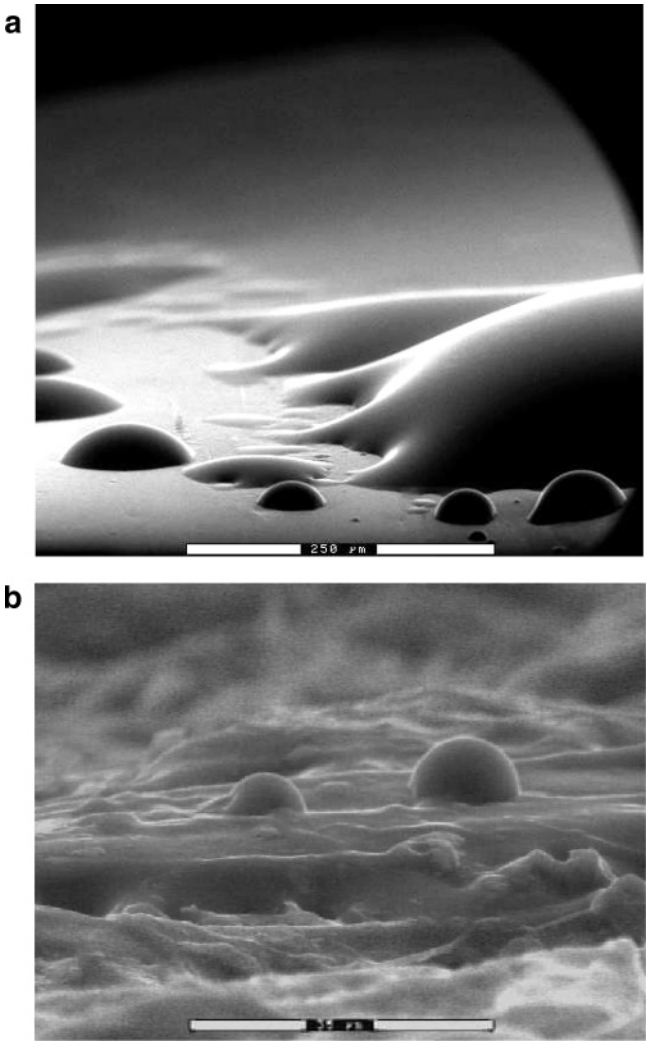


**Figure 3.** (a) ESEM image of droplets formed on a cellulose film. (b) ESEM image of droplets formed on newsprint paper.

Other possible sources of experimental uncertainty are the heating effect as well as the effect of the electric field. The electron beam of ESEM heats the sample locally, but there are unfortunately no quantitative reports on the possible magnitude of this effect. Bateni et al. (2005)[39] have reported on an approximately 0.5° variation of the contact angle of macroscopical droplets consisting of polar molecules (alcohols) on Teflon in an electric field on the order of magnitude of $10^6$ V/m. We assume that the electric effects in ESEM may have a minor effect (of a magnitude of 1°) on the contact angles in our system.

## 4. Results and Discussion

An optical inspection of the pictures obtained by the ESEM device shows that in most cases our theoretical approach stating that a liquid droplet is part of a sphere on a flat surface is correct (Figure 3a and b). In Figure 3a, droplets have formed on cellulose film, and the surface in Figure 3b represents newsprint paper. Even though the paper has a very complex structure, on the scale of a maximum of a few micrometers the surface can be considered to be rather flat. On the nanometer scale, which is relevant for the nucleation phenomenon, this approach can be considered to

(33) Kulmala, M.; Vesala, T.; Kalkkinen, J. *Data for Phase Transitions in Aerosol Systems*; University of Helsinki: Helsinki, Finland, 1990.

(34) Yaws, C. L., Ed. *Chemical Properties Handbook*; McGraw-Hill: New York, 1999.

(35) Lindsey, A. L.; Bromley, L. A. *Ind. Eng. Chem.* **1950**, *42*, 1508−1511.

(36) Fuchs, N. A.; Sutugin, A. G. *Highly Dispersed Aerosols.*; Ann Arbor Science Publishers: Ann Arbor, MI, 1970.

(37) Niskanen, K., Ed.; *Paper Physics*; Papermaking Science and Technology; Finnish Paper Engineers' Association and TAPPI: Helsinki, 1998; Book 16.

(38) Cameron, R. E.; Donald, A. M. *J. Microsc.* **1994**, *173*, 227−237.

(39) Bateni, A.; Laughton, S.; Tavana, H.; Susnar, S. S.; Amirfazli, A.; Neumann, A. W. *J. Colloid Interface Sci.* **2005**, *283*, 215−222.

**Table 1. Experimental Onset Saturation Ratios and Contact Angles Corresponding to the Classical Theory of Heterogeneous Nucleation for Different Materials at Different Temperatures**

| material | onset saturation ratio | temperature (°C) | corresponding contact angle (deg) |
|---|---|---|---|
| newsprint paper | 1.09 | 2.7 | $20.2 \pm 0.5$ |
| | 1.11 | 7.1 | $22.7 \pm 0.5$ |
| Teflon | 1.04 | 3.7 | $13.5 \pm 0.3$ |
| | 1.03 | 6.7 | $11.8 \pm 0.3$ |
| cellophane | 1.07 | 2.1 | $17.7 \pm 0.4$ |

be rather approximative. However, the limitations of the ESEM accuracy in this study leaves the considerations of the newsprint paper nanostructure for future inspection, and the flat surface approximation has also been made in the heterogeneous nucleation calculations.

Supersaturations leading to the onset of heterogeneous nucleation of water vapor were determined experimentally for newsprint paper, Teflon, and cellulose film. The contact angle and growth rate were measured for droplets on newsprint paper.

The experimental results for onset saturation ratios are shown in Table 1. For the model runs, the onset of nucleation was defined as the nucleation rate corresponding to the number concentration of observed droplets on the surface ($10^6$ cm$^{-2}$) divided by the time interval of the ESEM pictures (30 s). Table 1 also shows the contact angles obtained by matching the parameters in the nucleation rate calculations using eq 8 with the experiments to get the onset nucleation rate of $J_{onset} = 3.33 \times 10^5$ cm$^{-2}$ s$^{-1}$. A similar angle-fitting procedure has been performed by Wagner[40] for the heterogeneous nucleation of water and *n*-propanol on the surface of Ag particles. Inclusion of the surface diffusion in the nucleation rate calculation is expected to increase the theoretical nucleation rates by approximately 3 orders of magnitude in our temperature range.[41] We have included this effect in the error estimate of the contact angle.

The experimental results for the contact angle and droplet growth rate were $(69 \pm 2)°$ and $(0.07 \pm 0.02)$ $\mu$m/s, respectively. It should be pointed out that sizes around the critical cluster were below the resolution of the ESEM device used in the experiments.

Droplet growth was modeled using eqs 12−25. In the model calculations, the droplet density on the paper surface was assumed to be approximately $10^6$ cm$^{-2}$ on the basis of the experimental observations. The results of the model calculations and the experimentally observed droplet growth are presented in Figure 4. The black lines represent the modeled curves (solid line, no air is present; dashed line, 5 Torr of air is present), and the gray dashed−dotted lines refer to droplet growth observed with ESEM. The results indicate that the used condensation theory predicts considerably faster droplet growth than that observed experimentally. The predicted equilibrium sizes, however, are in rather good agreement with the experiments. A possible reason for the wrong time scale predicted by the model might be the fact that the water absorption of the paper fibers was not taken into account in the calculations. It is probable that the fibers absorb water first from the base of the droplets and second directly from the vapor phase, thereby slowing down the observed growth of the droplets.

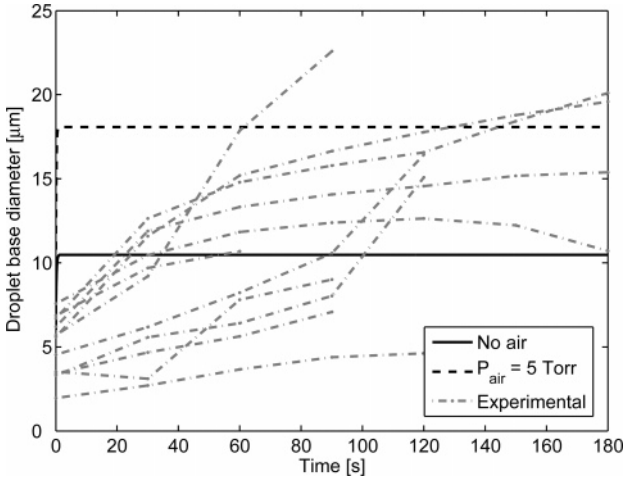


**Figure 4.** Time evolution of the size of a water droplet on a newprint paper surface. The gray dashed−dotted lines correspond to experimental results obtained during a single ESEM measurement. The solid line shows the result modeled using diffusion theory in the transition regime and assuming no carrier gas (calculated with eq 12), whereas the dashed line corresponds to model calculations assuming 5 Torr of air to be present in the gas phase (eq 15). The droplet temperature is considered to be the same as the underlying surface temperature in the beginning of the experiment, 275.85 K. The vapor temperature is 293.15 K.

## 5. Conclusions

The measured onset supersaturations were smaller than the modeled ones when the experimentally determined contact angle was used in the classical theory of heterogeneous nucleation. A better model result was gained using a smaller contact angle. The resolution of the ESEM device does not extend down to the diameter of critical size embryos, which is about 4 nm, so the experimentally determined contact angle possibly applies only for larger droplets.

The measured condensational growth rates were significantly slower than the modeled ones. This may be due to several approximations considering the topology and other attributes of the surface. One of the most important uncertainties relates to the probable mass transfer between the droplet base and the paper surface, namely, the water absorption by the paper fibers.

**Acknowledgment.** We thank Tiina Pöhler and Asko Sneck at KCL Science and Consulting for their efforts in the ESEM experiment and data analysis.

LA062073N

(40) Wagner, P.; Kaller, D.; Vrtala, A.; Lauri, A.; Kulmala, M.; Laaksonen, A. *Phys. Rev. E* **2003**, *67*, 021605.
(41) Seki, J.; Hasegawa, H. *Astrophys. Space Sci.* **1983**, *94*, 177−189.